Excited States of Bridged [14]Annulenes with Anthracene Perimeter: Absorption, Polarized Emission, Linear Dichroism, and Magnetic Circular Dichroism

Jaroslav Kolc,[1a] Josef Michl,*[1a,b] and Emanuel Vogel[1c]

Contribution from the Department of Chemistry, University of Utah, Salt Lake City, Utah 84112, and the Institute for Organic Chemistry, University of Cologne, Cologne, Germany. *Received July 14, 1975*

Abstract: The title methods were used to detect and assign seven electronic transitions below 35 000 cm^{-1} in a series of bridged [14]annulenes (I–IV) with gradually decreasing deviation from planarity. Four of the transitions can be correlated with those of anthracene and the series provides a partial concrete realization of Platt and Moffitt's theoretical model for deriving electronic states of polycyclic hydrocarbons from those of an annulene by introduction of transannular cross-links. The other three transitions involve states which cannot be simply related to π-electron states of [14]annulene. Comparison with results for dicyclohepta[*cd,gh*]pentalene (V) indicates that they originate in strong hyperconjugative interactions between the "π-orbitals" of the perimeter and "σ-orbitals" of the saturated bridge present in I–IV. The existence of such hyperconjugative interactions is also reflected in the observed absolute signs of the intense bands in MCD spectra.

The effect of distortions from planarity on the properties of conjugated π-electron systems has long been a subject of considerable interest to the organic chemist. In this context, much attention has focussed on ultraviolet–visible spectroscopy, which provides a fairly sensitive probe for the investigation of such distortions. It was recognized quite early from studies of polyenes that twisting along "essential double bonds" causes a red shift of $\pi\pi^*$ transitions present in the planar parent system, while twisting along "essential single bonds" has the opposite effect, and this is readily understood in terms of simple MO theories.

Twisting along "aromatic" bonds which form part of a conjugated ring structure has been studied less. The uv absorption bands of [*n*]paracyclophanes move to longer wavelengths as *n* is decreased, in agreement with π-electron calculations.[2] For ring systems of other sizes, similar series of compounds with gradually increasing deviations from planarity have not been available. The excitation energies of a bridged [10]annulene, for which a completely planar model is not at hand, could be accounted for when ring bending, calculated to have a lowering effect on the excitation energies, as well as transannular interaction, calculated to have the opposite effect, were both considered.[3]

Recent synthetic advances[4] in the field of bridged [14]-annulenes with anthracene perimeter put at our disposal a series of compounds I–IV well suited for an investigation of the

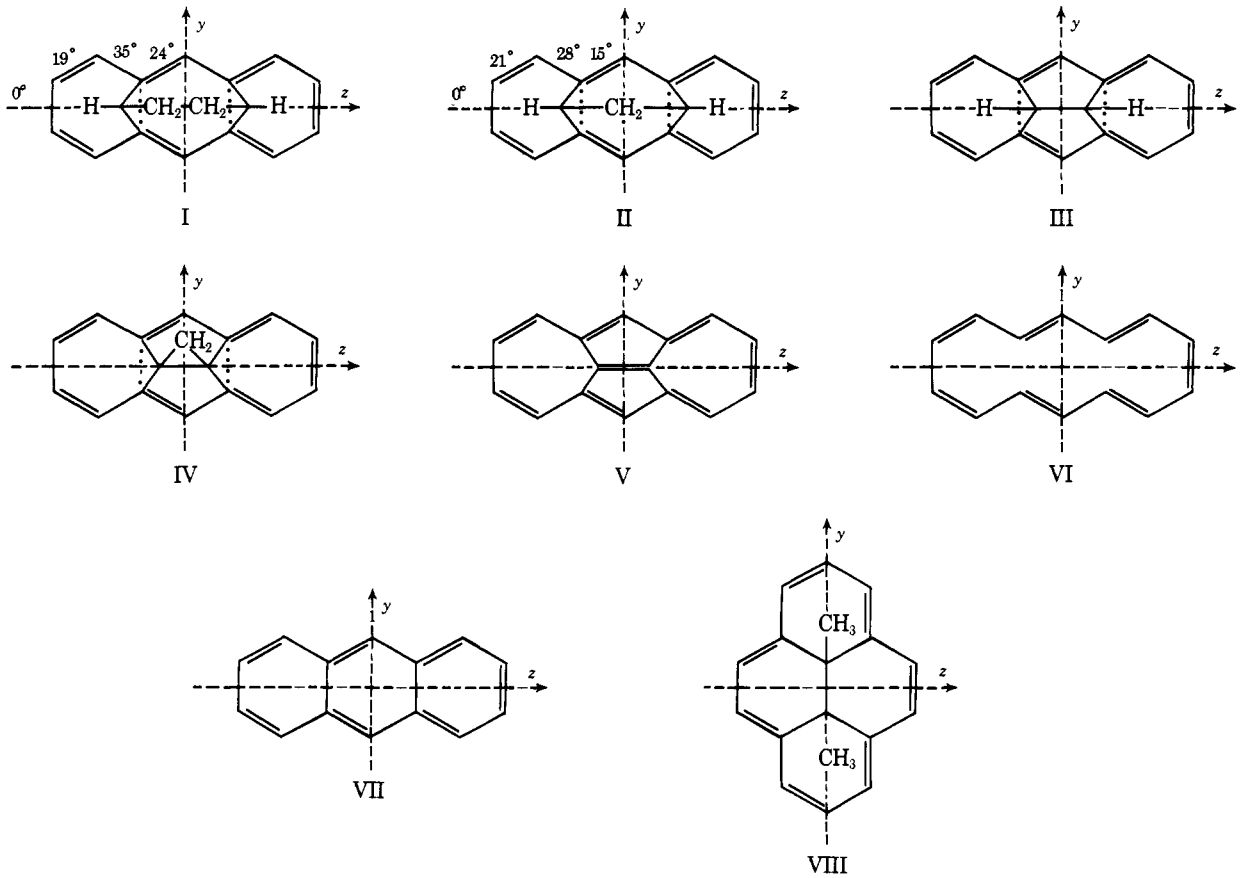

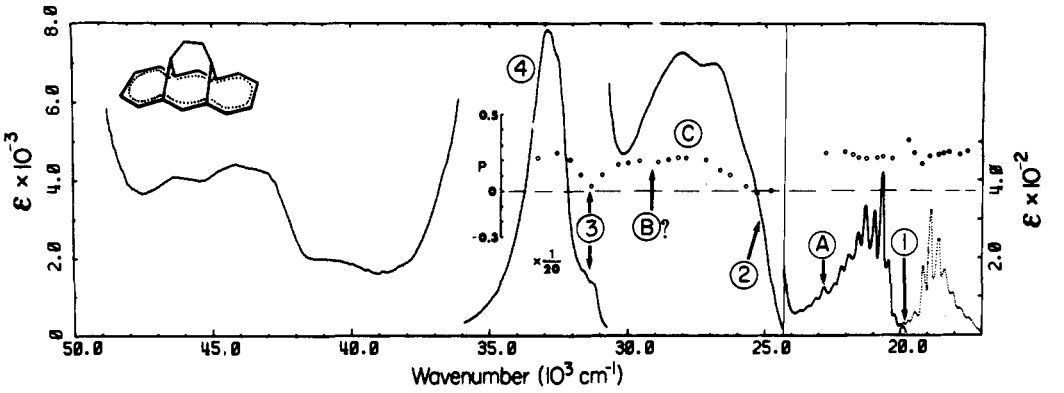

Figure 1. Butano-bridged [14]annulene I. Absorption (full line), emission (dotted line, not corrected for instrumental response), and degree P of polarization of excitation (empty circles) and emission (full circles) at 77 K in 3-methylpentane glass.

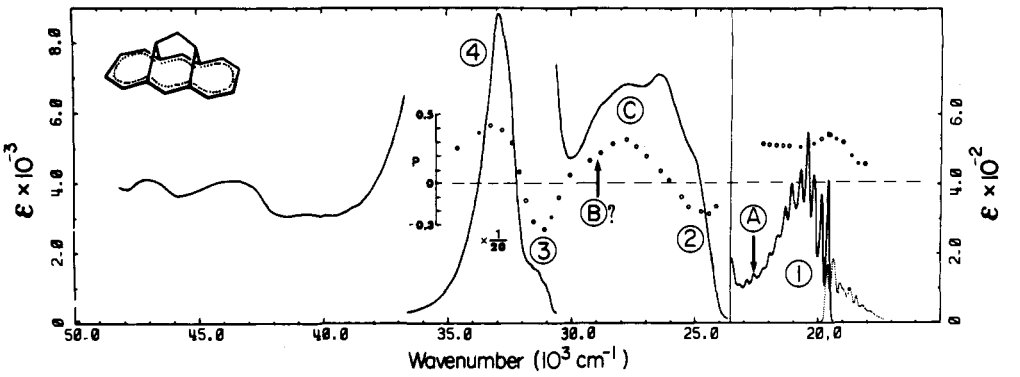

Figure 2. Propano-bridged [14]annulene II. See caption to Figure 1.

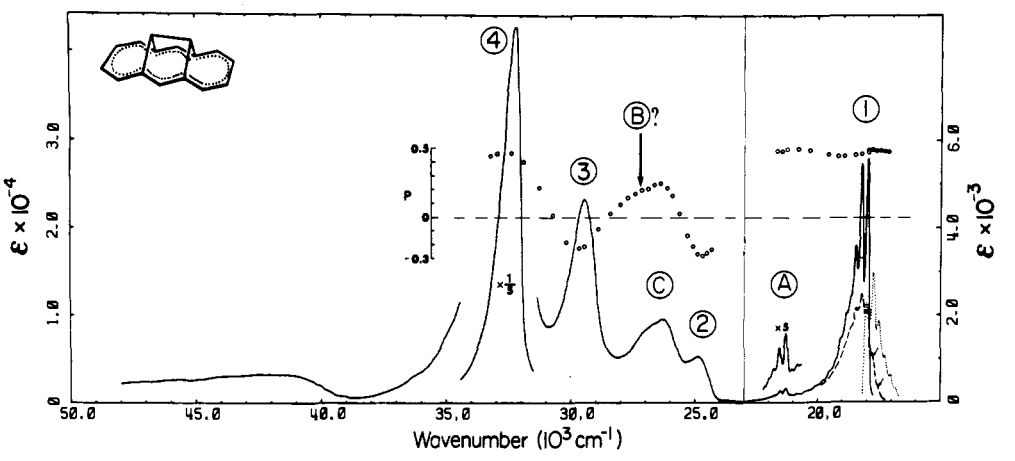

Figure 3. Ethano-bridged [14]annulene III. See caption to Figure 1. The dashed line represents the first absorption band at room temperature, arrows point to hot bands.

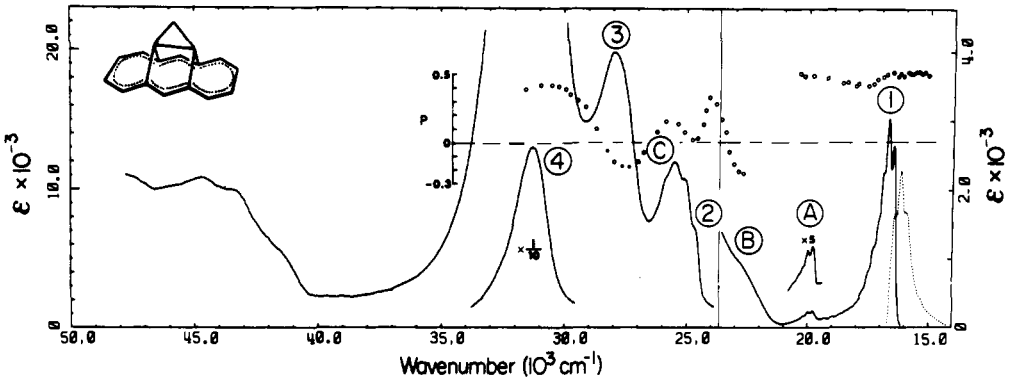

Figure 4. Cyclopropano-bridged [14]annulene IV. See caption to Figure 1.

effect of nonplanarity on spectroscopic properties. Comparison can also be made with the fully conjugated hydrocarbon V, whose electronic spectrum has been analyzed in detail elsewhere.[5] In the present paper, we report a detailed investigation of electronically excited states of I–IV. An NMR study of these molecules[6] and an investigation of their photoelectron spectra[7] and ESR spectra of their radical ions[8] have been reported separately.

Experimental Section

Materials. Preparation of pure samples of I–V has been described elsewhere.[4] 3-Methylpentane (3-MP, Phillips Petroleum Co.) was refluxed with sodium, distilled, and passed over an Al_2O_3–$AgNO_3$ column. Other solvents were spectral grade quality.

Absorption spectra in rigid glass (3-MP, 77 K) were taken in 2-mm Suprasil and 30-mm Pyrex cells immersed in a quartz Dewar with Suprasil windows, filled with filtered liquid nitrogen, using a Cary 17 spectrophotometer.

Linear dichroism was measured in stretched sheets of a copolymer of ethylene and vinyl acetate, transparent up to 40 000 cm^{-1}, which had been soaked in a saturated solution of the hydrocarbon in chloroform or ethyl acetate, air-dried, and rinsed with methanol to remove crystals from the surface. The sheet was immersed in liquid nitrogen inside a quartz Dewar with Suprasil windows. The optical path contained a rotatable Glan prism with polarization plane at ±45° from the vertical, ensuring approximately the same light flux for the measurement of the parallel ($E_\parallel$) and perpendicular ($E_\perp$) dichroic curve. The measurements were taken on a Cary 17 spectrophotometer interfaced to a PDP-11/20 computer. A more detailed description of the low-temperature equipment has appeared elsewhere.[9]

Polarized fluorescence and fluorescence excitation spectra were recorded in 3-MP rigid glass at 77 K using an instrument described previously.[10]

Magnetic circular dichroism was measured in cyclohexane at room temperature as described in ref 11.

Results

The spectra of ordinary low-temperature absorption and fluorescence of hydrocarbons I–IV are shown in Figures 1–4. The degree of polarization in emission as well as excitation spectra (P) is also displayed. Excitation spectra followed faithfully the details of the absorption spectra in each case. The low-temperature absorption curve[5] of V is shown in Figure 5.

Measured curves of linear dichroic absorption $E_\parallel$ and $E_\perp$ showed that in each case the very strong absorption peak near 33 000 cm^{-1} is polarized along the long axis of the molecule, while the weaker peak or shoulder on its low-energy side is polarized along one of the two short axes. From consideration of molecular shape, we identify the long axis with the z axis in formulas I–V, leaving the y and x (out of plane of paper) axes as the "short" ones. As an example, Figure 6 presents the experimental curves $E_\parallel$ and $E_\perp$, corrected for baseline, for the ethano annulene III.

The experimental curves were combined to obtain the "reduced absorption curves" corresponding to pure long and short axis polarizations, using the usual stepwise reduction procedure.[12] Since all short-axis polarized peaks disappear from the linear combination $A_z = E_\parallel - d_\parallel^\circ E_\perp$ simultaneously when a suitable value of $d_\parallel^\circ$ is found by trial and error, they are either all polarized along only one of the two short axes, presumably the one labeled y in formulas I–IV (by analogy to the planar hydrocarbon V, in which we do not expect other than $\pi\pi^*$ transitions to occur below 35 000 cm^{-1}), or the orientation distribution is such that the two axes are equivalent, or both. We shall see later that the equivalence of the two axes indeed obtains in the case of hydrocarbons I–III. The reduced curve for short-axis polarized absorption is obtained as $A_y = n_0(E_\perp - d_\perp^\circ E_\parallel)$. Here we use the label A_y although, in principle, some of the peaks may actually be polarized along x in molecules I, II, and III.[12b] The normalization factor n_0 was obtained from the formula[12a] $n_0 = (2 + d_\parallel^\circ)/(2d_\perp^\circ + 1)$. The reduction factors $d_\perp^\circ$ and $d_\parallel^\circ$, which reflect the molecular orientation distribution in the stretched polymer, were $d_\perp^\circ = 0.77$, $d_\parallel^\circ = 0.87$ for I; $d_\perp^\circ = 0.70$, $d_\parallel^\circ = 0.80$ for II; $d_\perp^\circ = 0.30$, $d_\parallel^\circ = 0.50$ for III; and $d_\perp^\circ = 0.43$, $d_\parallel^\circ = 0.95$ for IV. These values are to be compared with those obtained[5] for V under the same experimental conditions: $d_\perp^\circ = 0.35$, $d_\parallel^\circ = 0.80$.

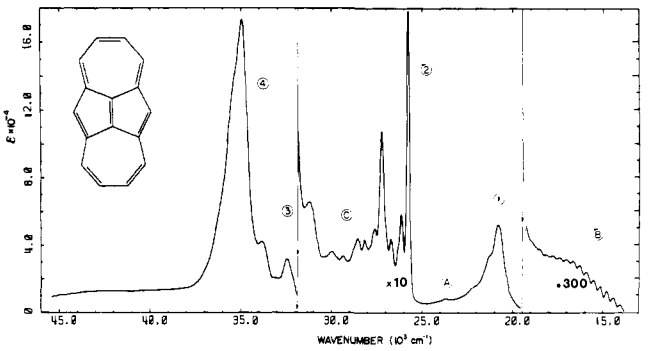

Figure 5. Absorption[5] of dicyclohepta[*cd,gh*]pentalene V in 3-methylpentane glass at 77 K.

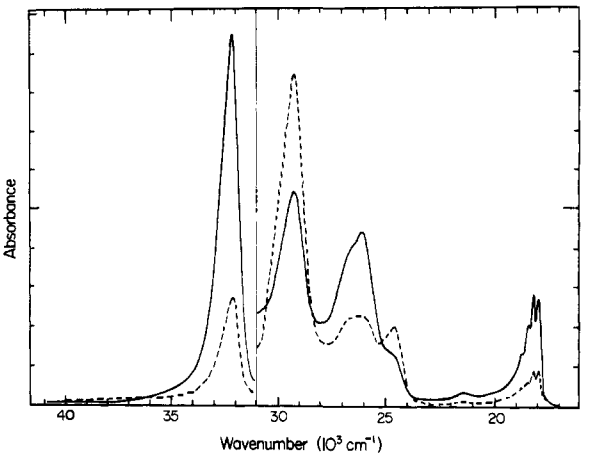

Figure 6. Ethano-bridged [14]annulene III. Dichroic absorption curves in a stretched copolymer at 77 K (see text). Full line: parallel spectrum $E_\parallel$, dashed line: perpendicular spectrum $E_\perp$.

The resulting reduced polarized spectra for hydrocarbons I–IV are shown in Figures 7–10, which also show the magnetic circular dichroic (MCD) spectra of these hydrocarbons. The region of the very weak first absorption band is missing in the case of I (Figure 7) owing to its limited solubility in the polymer sheet. For the purpose of comparison of spectral shapes in the discussion which follows, we also reproduce the corresponding published[5] spectra for the fully conjugated analogue V (Figure 11).

The measurements on II were repeated in stretched polyethylene and polypropylene sheets. The same reduced polarized spectra resulted.

Discussion

A. Absorption and Emission Spectra. Although the absorption spectra of the bridged [14]annulenes I–IV each exhibit distinct characteristics of their own, their overall similarity is unmistakable (Figures 1–4). Many individual electronic transitions could be identified and traced throughout the series I–IV on the basis of the low-temperature absorption curves alone. The additional spectral information available makes such a task much easier and increases our confidence in the correctness of the assignment. We shall, therefore, return to the problem of band assignment after a brief discussion of the auxiliary spectroscopic methods.

Only one feature will be pointed out here, namely the ob-

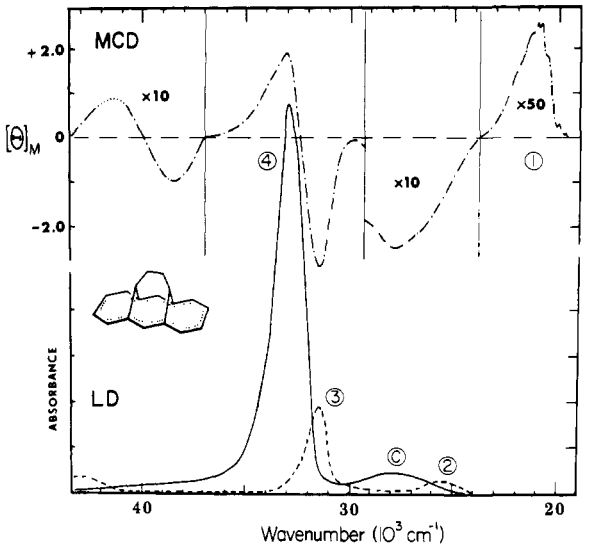

Figure 7. Butano-bridged [14]annulene I. Reduced absorption spectra (stretched copolymer of vinyl acetate and ethylene, 77 K): long-axis polarized (full line) and short-axis polarized (dashed line). Both spectra on the same scale of absorbance (arbitrary units). Magnetic circular dichroism (cyclohexane, room temperature) dash-dot line. Molar ellipticity per unit field strength in units of deg l. m^{-1} mol^{-1} G^{-1}.

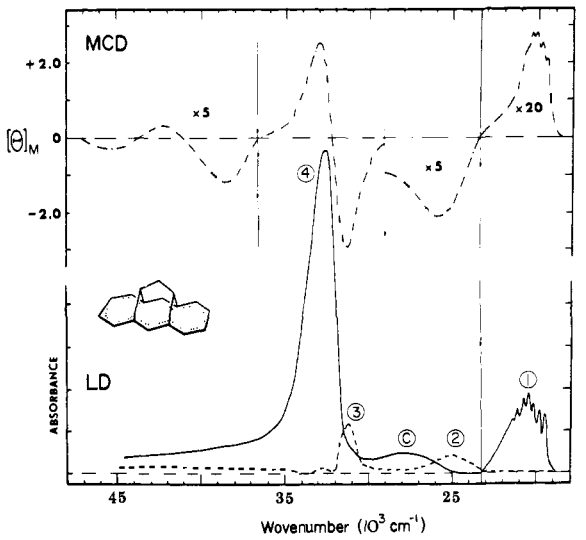

Figure 8. Propano-bridged [14]annulene II. See caption to Figure 7. Note different scales for absorbance below and above 23 200 cm^{-1}.

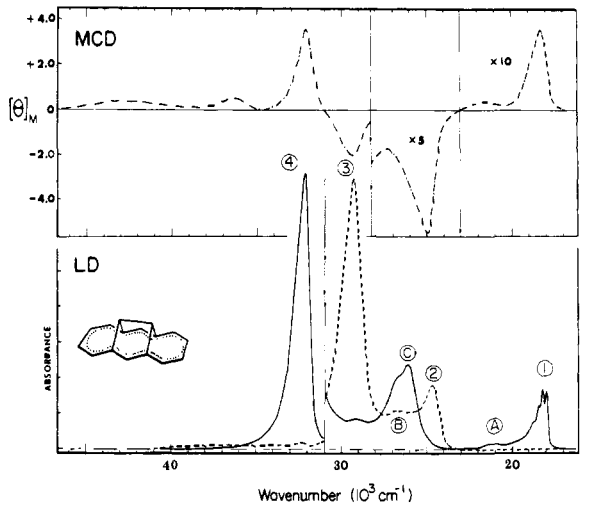

Figure 9. Ethano-bridged [14]annulene III. See caption to Figure 7. Note different scales for absorbance below and above 31 000 cm^{-1}.

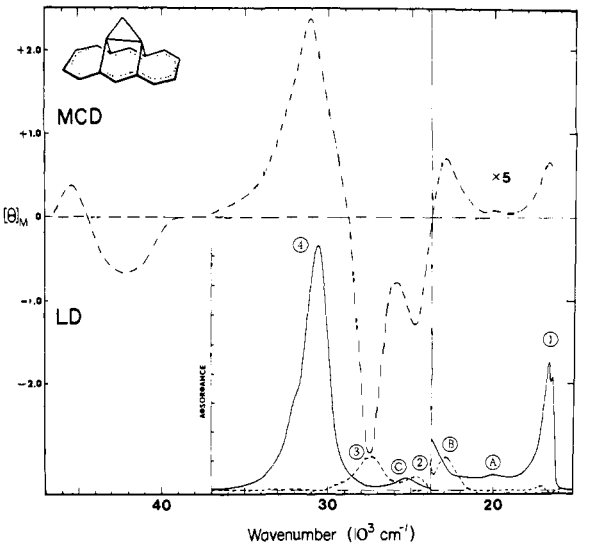

Figure 10. Cyclopropano-bridged [14]annulene IV. See caption to Figure 7. Note different scales for absorbance below and above 23 800 cm^{-1}.

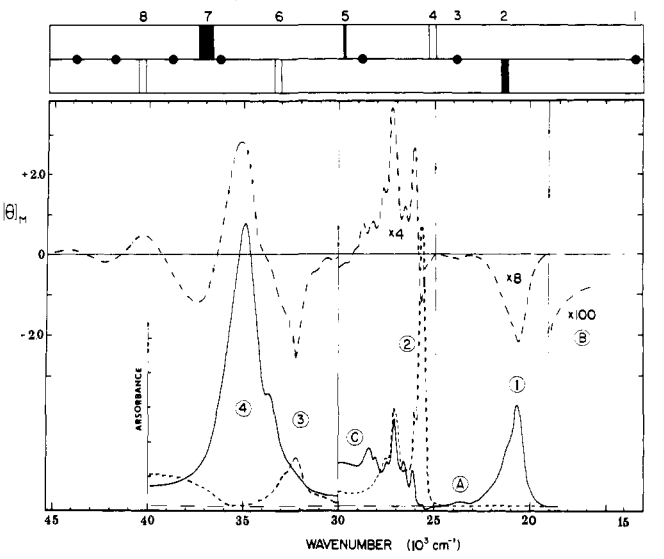

Figure 11. Dicyclohepta[*cd*,*gh*]pentalene[5] V. See caption to Figure 7. Note different scales for absorbance below and above 30 000 cm^{-1}. PPP-SECI-I calculations from ref 5 are shown on top: long-axis polarized (black), short-axis polarized (white), and symmetry-forbidden (dot) transitions of small (thin line), medium (medium line), and high (thick line) intensity. Transitions shown in lower (upper) strip are calculated to appear as negative (positive) peaks in MCD spectrum.

servation of distinct hot bands in room-temperature absorption and emission of hydrocarbons II, III, and IV, unusual in solution spectra of molecules of this size. The long-wavelength part of absorption as well as emission are highly structured in spectra taken at 77 K (Figures 1–4), and their 0–0 bands coincide. In spectra taken at room temperature, the fine structure is less well developed, and hot bands clearly appear, with expected intensity (only a broad tail is observed for I). The room temperature absorption curve of III is displayed in Figure 3 and hot bands are indicated by arrows. Their distinct appearance is undoubtedly due to the availability of a single vibration of very low frequency (200–300 cm^{-1}), which is also observed in the fine structure of emission, and to the Franck–Condon allowed shape of the absorption bands. It appears likely that this low-frequency vibration corresponds to a totally symmetrical "out-of-plane" deformation of the ring of carbon atoms in the annulenes.

B. Orientation in Stretched Copolymer Sheet. For the purposes of linear dichroic spectroscopy, the molecular orientation

distribution in a uniaxially stretched polymer can be characterized[12] by two orientation factors, $K_1 = \langle\cos^2\beta\rangle_{av}$ and $K_2 = \langle\sin^2\beta\cdot\cos^2\gamma\rangle_{av}$. Here, β and γ are two of the Euler angles used to describe molecular orientation; β measures the deviation of the long axis of the molecule from the stretching direction while γ measures the rotation of the molecule along its own long axis. If γ equals 0 or 180° for a planar molecule, its short in-plane axis lies in the plane containing the long axis and the stretching direction. Alternatively, K_2 can be expressed in terms of the angle β' between the "longer" of the short axes, y, and the stretching direction: $K_2 = \langle\cos^2\beta'\rangle_{av}$.

The orientation factors can be obtained from the reduction factors $d_{\parallel}°$ and $d_{\perp}°$.[12] Their values for hydrocarbons I–V are collected in Table I. The degree of alignment of the long axis, given by K_1, is seen to increase dramatically as one goes from the strongly bent[13] butano derivative I to the less bent[14] propano derivative II and on to III which, according to models, has an almost planar conjugated perimeter. When the bridge is also pushed into the plane of the perimeter (V), K_1 remains almost unchanged. When the bridge is made bulkier (IV), the orientation becomes worse. All of these trends appear qualitatively quite reasonable, using the simple rule "solutes prefer to expose their smallest cross-section in the stretching direction".

The physical interpretation of the values of K_2 is more complicated. If the distribution of angles γ is uniform, i.e., all angles of rotation of the molecule along its long axis are equally probable, it can be shown[12] that K_1 and K_2 are related by $K_2 = (1 - K_1)/2$. This situation will clearly obtain for molecules with cylindrical symmetry, such as acetylene, and is assumed by some authors to prevail universally. Stretched sheet results available to date indicate that approximately uniform γ-distribution is obtained with molecules such as anthracene, tetracene, and others with approximately rod-like shape, but not with pyrene, perylene, fluoranthene, azulene, and other molecules with a more or less sheet-like shape.[9,10,12] In the latter, preferred orientation in a stretched polymer is such that the edge rather than the flat side of the sheet is exposed when viewing along the stretching direction (of course, for those molecules whose long axis happens to be perfectly aligned with the stretching direction, the edge is exposed for any value of γ).

Comparison of the values of K_2 with $(1 - K_1)/2$ in Table I shows that I, II, and III have no clearly preferred rotation angle along their long axis. This is again understandable on the basis of molecular shapes. The presumably completely planar hydrocarbon V prefers to orient similarly as other sheet-shaped molecules, exposing its edge rather than its flat side when viewed along the stretching direction. Surprisingly, IV behaves in the same way, although its bridge is higher and bulkier than that of III, at least if one makes the very plausible assumption that the observed short-axis polarized absorption is polarized along the y axis rather than the x axis in formula IV. Apparently, details of the shape of the bridge play an unsuspected role.

In summary, most of the observed regularities in the orientation characteristics can be rationalized by simple-minded consideration of molecular models, but details of the orientation behavior of nonplanar molecules are presently not predictable.

C. Polarized Emission. The observed degree of polarization in emission and excitation shows an interesting trend (Figures 1–4). For III and IV, and to a slightly lesser degree, II, the plots shown are textbook examples in that the polarization degree ranges from very near its theoretical upper limit (+½) to very near its theoretical lower limit (−⅓), pinpointing transitions polarized parallel and perpendicular to the polarization of the transition to the lowest excited state, respectively, in excellent agreement with the stretched sheet spectra (Figures 8–10). On the other hand, the curve for 1, which was obtained under identical experimental conditions, is noticeably flatter and the theoretical limits are not reached. Fortunately, tentative conclusions about polarization directions can still be reached, and they again agree with the stretched sheet spectra (Figure 7).

Table I. Orientation Factors[12] of Bridged [14]Annulenes in Stretched Sheet

	I	II	III	IV	V
K_1	0.39	0.42	0.63	0.54	0.59
K_2	0.30	0.29	0.20	0.32	0.29
$(1 - K_1)/2$	0.30	0.29	0.19	0.23	0.21

The difference can be only partly ascribed to a higher degree of band overlap in I. We suspect that it is related to the fact that among I–IV, only I has a strongly Franck–Condon forbidden first transition (in absorption as well as emission). This indicates a larger difference of geometry for this molecule between the ground and lowest excited singlet states. Sizable interactions with the neighboring molecules in the rigid glass may well result if the molecule bends more or becomes flatter, and these may lead to an overall rotation of the molecule before it fluoresces, and thus to depolarization of the emitted light. Probably more important, a lowering of molecular symmetry upon excitation is a likely possibility. For I, but not II, III, and IV, molecular models indicate a relatively facile twisting motion which removes the eclipsing interactions on the $-CH_2-CH_2-$ portion of the butano bridge. This relief is apparently not operative in the ground state, which has been found[13] to have C_{2v} symmetry, presumably since it would involve further disruption of the already nonplanar aromatic annulene ring. However, it should occur more easily in $\pi-\pi^*$ excited singlet states, in which π-bonding is weakened.

D. Magnetic Circular Dichroism. In the present paper, we use MCD spectra mostly in a very crude fashion, namely to help to identify and characterize individual electronic transitions. This is based on the well-known experimental fact that MCD bands generally follow the shape of absorption bands, except that they can be negative as well as positive, and that the relative intensities in MCD need not be the same as in absorption. This correspondence between MCD and absorption spectra can be justified theoretically in the absence of vibronic interactions,[15] and its absence indicates the existence of such interactions (e.g., in azulene[9]).

A complete exploitation of the information contained in the MCD curves is best based on calculations, at least approximate, and is outside the scope of this paper. Nevertheless, we will take advantage of the fact that a Pariser–Parr–Pople (PPP) type π-electron calculation similar to those used successfully to account for absolute signs in the MCD spectra of other hydrocarbons,[9,10,16] including V,[5] gives vanishing MCD intensities for any electroneutral even alternant hydrocarbon such as the hypothetical planar [14]annulene with anthracene perimeter (VI). This is perhaps most easily seen from the fact that, in the sense of alternant symmetry, such a hydrocarbon is paired with itself in the PPP model, while a general theorem demands[17] that MCD spectra of any two species paired by alternant symmetry be equal in magnitude and opposite in sign. The observed signs in the MCD spectra of the bridged annulenes I–IV will then provide information about the nature of perturbations introduced by the bridge.

Finally, let us mention that MCD spectra of other bridged annulenes have been published[18] and that it was noted that they are quite sensitive to details of the structure of the bridge and to substitution. This is understandable in view of the above remarks. The similarity of the MCD spectra of hydrocarbons I–IV (Figures 7–10) reflects the homogeneity of this series of [14]annulenes. On the other hand, the signs of many of the

Table II. Spectroscopy of Bridged [14]Annulenes[a]

		Transition						
		1	A	2	B	C	3	4
I	E	19.84	22.80	25.5	29.5(?)	28	31.5	33.0
	f	0.003	~0.0002	0.04	~0	0.11	0.21	1.2
	pol	z	z	⊥	⊥	z	⊥	z
	B	−0.1	~0		+1		+3	−3
II	E	19.57	22.57	25	29(?)	27.5	31.1	33.0
	f	0.004	~0.0001	0.06	~0	0.09	0.15	1.6
	pol	z	z	⊥	⊥	z	⊥	z
	B	−0.4	~0		+1.5		+3.5	−3
III	E	17.99	21.29	24.8	27	26.2	29.5	32.2
	f	0.020	~0.0004	0.02	0.08		0.15	1.1
	pol	z	z	⊥	⊥	z	⊥	z
	B	−0.6	−0.1	+3		~0	+3	−4
IV	E	16.43	19.76	24.5	23	25.2	27.5	31.0
	f	0.013	~0.0003	0.03	0.008	0.03	0.13	1.3
	pol	z	z	⊥	⊥	z	⊥	z
	B	−0.3	−0.02	+2.4	−0.3	~0	+5	−7

[a] Excitation energy of the 0–0 band in units of 10^3 cm^{-1} (E), oscillator strength $f = 4.319 \times 10^{-9} \int \epsilon \, d\nu$ (using polarized spectra to estimate areas of overlapping bands), polarization (along z axis or perpendicular to it), and B term in units $10^{-3} \beta_e$ D^2/cm^{-1}, obtained from $B = -(33.53\nu_0)^{-1} \int [\theta]_M \, d\nu$, where ν_0 is the wavenumber of the band center.

MCD bands of the related fully conjugated 16 π-electron hydrocarbon V are distinctly different (Figure 11).

E. Identification of Electronic Transitions. Combining the results of all spectroscopic methods (Figures 1–4 and 7–10), we believe that seven distinct electronic transitions can be assigned in the region below 35 000 cm^{-1} (Table II). Most of the these can be found in all four hydrocarbons I–IV. We shall label them in two separate groups for reasons which will become clear later: 1 through 4 in the order of increasing energy, and A through C, again in the order of increasing energy (the order of B and C is reversed in IV). A survey of assignments in all four compounds is given in Figure 12 and in Table II.

Transition 1. This is the only transition for which the energy of the 0–0 component can be measured quite accurately. It decreases regularly from I to IV. The intensity changes dramatically along the series. At 77 K, the decadic molar extinction coefficients of the most intense peaks (ϵ_{max}) are 415, 560, 5500, and 3000 for I, II, III, and IV, respectively. The reduced spectra and polarized emission spectra show that transition 1 is purely long-axis polarized. It has a positive MCD peak. An unusually large number of totally symmetrical vibrations representing a variety of frequencies are active in its fine structure to about the same degree. This provides the band with characteristic very dense, yet distinct, vibrational structure. The band of transition 1 is Franck–Condon allowed and quite narrow in III and IV (half-width ca. 1000 cm^{-1}). In II and particularly I, the band has Franck–Condon forbidden shape and is about twice as wide. The case of I has already been discussed above. Clearly, III and IV do not change shape much upon excitation, while II and particularly I do. The totally symmetrical vibrations observed in absorption are 120, 260, 360, 570, 840, 1100, and 1450 cm^{-1} in I; 270, 590, 860, 1130, and 1500 cm^{-1} in II; 240, 460, 630, 820, 1030, and 1540 cm^{-1} in III; and 220, 430, 630, 810, 1020, and 1360 cm^{-1} in IV. Combination bands mostly involve one quantum of the highest of the frequencies. In each case, emission is a reasonable mirror image of absorption. The ground-state frequencies identified in emission are 130, 290, 350, 590, 880, 1120, and 1390 cm^{-1} in I; 240, 510, 690, 900, 1150, and 1420 cm^{-1} in II; 220, 430, 610, 850, and 1080 cm^{-1} in III; and 190 and 450 cm^{-1} in IV. Estimated error limits on these values are ±30 cm^{-1}. The very low frequency vibration observed in I but not the other hydrocarbons (120 cm^{-1}) can be tentatively identified with the torsional vibration discussed above. A higher resolution study will be necessary to permit definitive conclusions.

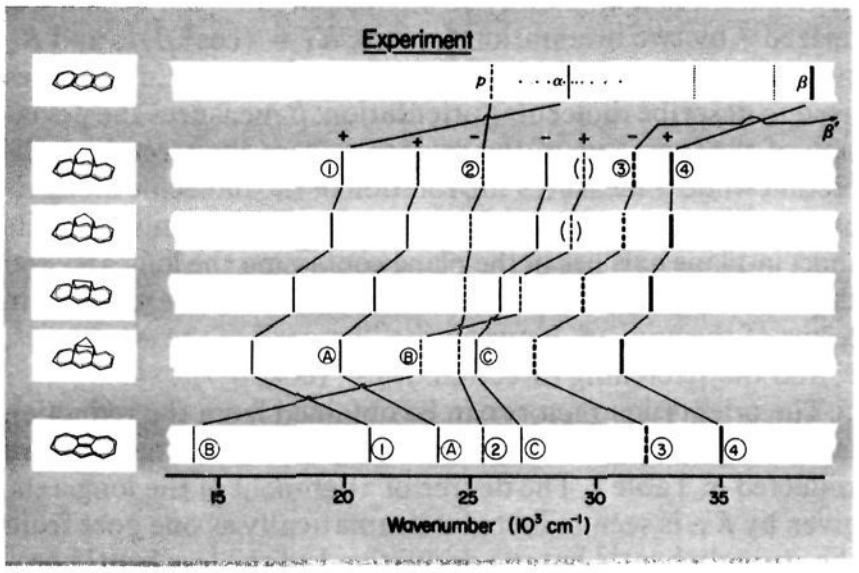

Figure 12. Correlation of observed transitions 1–4 and A–C in hydrocarbons I–V and VII. Full lines: long-axis polarized; dashed lines: short-axis polarized, dotted lines: symmetry-forbidden transitions. Thick lines: intense transitions; thin lines: weak transitions. MCD signs are indicated on top.

Transition 2. The energy of this medium intensity transition is about 24 500 cm^{-1}, and is remarkably constant throughout the series. The transition is negative in MCD. It is clearly short-axis polarized in reduced spectra, and is represented by a dip in the plot of the degree of polarization of fluorescence excitation (overlapping with a positive contribution from transition C in the case of IV).

Transition 3. The energy of this transition decreases very similarly as that of transition 1 upon going from I (ca. 31 500 cm^{-1}) to IV (ca. 28 000 cm^{-1}). This is the second strongest transition in the spectrum ($\epsilon_{max} \simeq 20\,000$), but since it is located quite close to the even much stronger transition 4, it appears only as an indistinct shoulder in the ordinary absorption spectra of I and II. It is, however, very distinct both in MCD spectra, where it appears as a strong negative peak, and in polarized spectra, which show that it is short-axis polarized. It is also clearly seen as a dip in the plots of the polarization degree P.

Transition 4. This is the most intense transition in the spectrum: ϵ_{max} is 158 000 (I), 180 000 (II), 210 000 (III), and 130 000 (IV). Its energy remains reasonably constant throughout the series (ca. 32 000 cm^{-1}), but not quite as much as that of transition 2. It is long-axis polarized and has a positive MCD peak.

Transition A. This is a striking but weaker replica of the first transition. There is no doubt that it is an intrinsic transition of the bridged annulenes and is not due to an impurity, since it clearly appears in the excitation spectra. It shifts to lower energies on going from I to IV just like transition 1 does and the separation of the first peaks of the two transitions is almost constant (3150 ± 200 cm^{-1}). In each of the four compounds, the same vibrational spacings are found in the first two transitions. The intensity of transition A is only a small fraction of that of transition 1 and is hard to estimate because of overlap with the tail of transition 1. It grows on going from I to III and then decreases somewhat on going to IV (ϵ_{max} I, 120; II, 140; III, 340; IV, 230), just like the intensity of transition 1 does, but the changes are not nearly as dramatic. The transition is long-axis polarized and positive in the MCD spectrum, and in this it again resembles transition 1.

Since transition A has such low intensity, and since the region of its true origin could be obscured by the tail of transition 1, we cannot be sure that the observed polarization is intrinsic. The observed origin on which vibrations already familiar from

transition 1 are built could be a false one, involving one vibration of a nontotally symmetric vibration and the observed intensity could be all borrowed from transition 1.

Transitions B and C. In addition to the transitions already discussed, the region 20 000–30 000 cm^{-1} contains at least two additional bands, one short-axis polarized and one long-axis polarized. On going through the series of compounds, they move independently of each other and also of the previously discussed transitions, and are therefore assigned as separate electronic transitions, B and C, respectively, rather than as vibronic intensity due to one or another of the transitions already discussed. The presence of two additional transitions is most obvious in the spectra of III and IV, while only one of them (C) can be clearly observed in the spectra of I and II.

The short-axis polarized transition B can be most clearly identified in the spectra of IV. In absorption, it appears as a distinct shoulder at 22 500 cm^{-1} ($\epsilon_{max} \simeq 1000$), and the corresponding negative dip in the curve of the degree of polarization (Figure 4). In the polarized spectrum it appears as a distinct peak near 23 000 cm^{-1}, and its presence is equally obvious in the MCD spectrum, where it is positive and about as strong as the peak of transition 1 (Figure 10).

One might argue that our assignment of transitions B and 2 in IV, which are both short-axis polarized, should be reversed. We prefer the assignment indicated, since it fits better with the approximately constant energies and intensities of transition 2 in the remaining compounds, and since this way the MCD peak of transition 2 in IV is negative, just as it is in all the others.

In the ethano compound III, the region between transitions A and 2 contains no shoulder or peak analogous to that assigned as B in IV. However, the polarized spectrum (Figure 9) shows a weak short-axis polarized peak near 27 000 cm^{-1}, corresponding to a slight but reproducible dip in the plot of the polarization degree P (Figure 3), and we assign this tentatively as transition B.

In hydrocarbons I and II, similar dips in the plot of P occur near 29 000 cm^{-1} (Figures 1, 2). The polarized curves are not sufficiently reliable in this region to provide much support (Figures 7, 8). Since we feel that the transition is certainly present in IV, and most likely in III, we guess but cannot be sure that it probably also occurs in I and II, and associate it very tentatively with the dips observed.

In contrast, the identification of the stronger long-axis polarized transition C presents no difficulties. It is always located between transitions 2 and 3 and, unlike the latter, must have a very weak MCD counterpart, since it usually cannot be discerned in the MCD spectrum at all. Only in the case of I is it clearly seen as a negative MCD peak. In the plots of the degree of polarization P, transition C is reflected as a clear region of positive values, in the middle of which there is the above-discussed dip due to transition B, or, in the case of IV, to transition 2. We have considered and rejected the possibility that band C is of vibronic origin and only represents intensity borrowed by the short-axis polarized transition 2 from the long-axis polarized intense transition 4. The argument against this is the variable separation of peaks assigned as 2 and C. This separation decreases regularly as one goes from I to IV. In IV, the origin of C already lies at a lower energy than the origin of 2, although the peak of C still is at higher energies than that of 2. This is seen in the polarized spectra in Figure 10, and, more clearly, in the plot of the polarization degree P shown in Figure 4, which is positive on both sides of the dip associated with transition 2. Since a false origin cannot be at lower energies than the true one, we conclude that the long-axis polarized intensity is not part of the vibronic structure of transition 2, but corresponds to a separate electronic transition.

Transitions of Higher Energies. The absorption and MCD spectra shown indicate the presence of several additional transitions above 35 000 cm^{-1}. Since they are poorly resolved, and since polarization data are missing, we feel that it is not profitable to attempt to discuss them in any detail at this time.

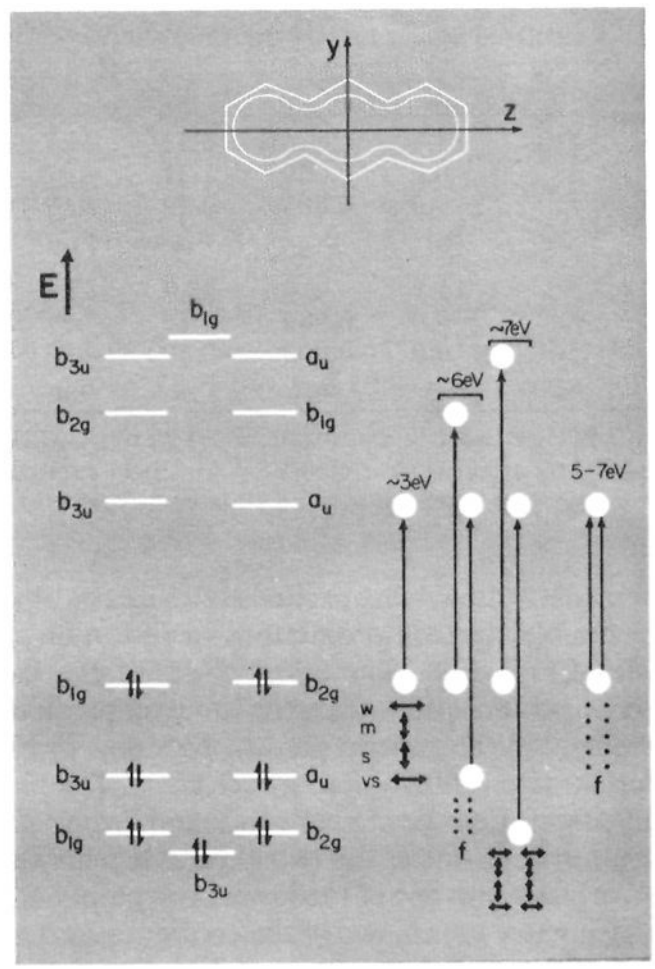

Figure 13. Molecular orbitals of [14]annulene VI, their ground state occupancy, and states resulting from first-order configuration interaction among singly excited singlet configurations. Number and polarization of transitions expected from each group of excitations is shown by arrows (dots labeled by f indicate symmetry-forbidden transitions).

F. Spectral Interpretations. X-ray crystallography[13,14] showed that I and II have C_{2v} symmetry and a quite regular periphery of "aromatic" C–C bonds. Molecular models suggest that the same will be true of III and IV, and that V is planar (D_{2h} symmetry). The best simple model on which a discussion of the states of the bridged annulenes I–IV can be based appears to be the hypothetical planar [14]annulene of D_{2h} symmetry shown in formula VI.

Low-lying electronic states of such a species should be of π–π^* character. Using the designation of axes shown in formula VI, their possible symmetries are A_g, B_{3g}, B_{1u}, and B_{2u}. Transitions from the A_g ground state to A_g and B_{3g} states are dipole forbidden, those to B_{1u} states are z-polarized, those to B_{2u} states are y-polarized. On going to the nonplanar C_{2v} molecules I–IV, only one axis of twofold symmetry remains. This is x in formulas I–IV; conventional labeling for it would be z, but in stretched sheet work, we keep the label z consistently for the long axis of the molecule. With our labeling convention, A_g, B_{3g}, B_{1u}, and B_{2u} states of VI become A_1, A_2, B_1, and B_2 states of I–IV. Transitions from the A_1 ground state to A_1 states are x-polarized, transitions to A_2 states are dipole forbidden, those to B_1 states are z-polarized, and those to B_2 states are y-polarized.

a. Hypothetical Planar [14]Annulene (VI). We shall assume that the states of I–IV which are of other than π–π^* parentage when derived from the hypothetical planar [14]annulene VI need not be considered since we are limiting ourselves to the region of low energies (up to 35 000 cm^{-1}).

The π-electron orbitals of a regular [14]annulene of D_{14h} symmetry are totally determined by symmetry. Those of a planar [14]annulene of D_{2h} symmetry, VI, are almost identical with the above. Their energies and symmetries, as well as ground state occupancy by the 14 π-electrons, are shown in Figure 13. They were obtained using the standard PPP π-

Table III. Calculated Spectrum of [14]Annulene VI[a]

		1	2	3	4	5	6	7	8	9	10	11	12	13
SCI[b]	E	15.8	21.6	30.2	34.1	35.9	38.8	41.6	44.5	44.6	45.0	47.5	50.2	50.4
	f_r	0.0	0.009	1.21	4.32	0.0	0.0	0.0	0.0	0.0	0.0	0.0	0.0	0.0
	f_p	0.0	0.006	0.29	1.19	0.0	0.0	0.0	0.0	0.0	0.0	0.0	0.0	0.0
	sym	B_{1u}	B_{2u}	B_{2u}	B_{1u}	A_g	B_{3g}	B_{3g}	A_g	B_{3g}	A_g	B_{3g}	B_{1u}	A_g
SECI-1[c]	E	15.9	22.0	28.7	32.9	36.8	36.9	38.3	38.5	40.7	40.8	41.2	41.7	44.1
	f_r	0.0	0.009	0.72	2.57	0.0	0.0	0.0	0.0	0.0	0.0	0.0	0.0	0.0
	f_p	0.0	0.006	0.59	2.08	0.0	0.0	0.0	0.0	0.0	0.0	0.0	0.0	0.0
	sym	B_{1u}	B_{2u}	B_{2u}	B_{1u}	A_g	B_{3g}	A_g	B_{3g}	A_g	B_{3g}	B_{3g}	A_g	A_g

[a] SCF–CI PPP method; E: transition energy in units of 10^3 cm^{-1}; f_r (f_p): oscillator strength obtained from dipole length (velocity) formula; sym: see labeling of axes in formula VI. [b] All singly excited configurations. [c] Selected singly and doubly excited configurations (133 in all). The SCF energy was taken for ground state energy; see text.

electron model.[19] Low-lying excited states can be obtained by single or double electron promotions as shown on the right-hand side of Figure 13. The exact values of energies of the various configurations depend on the values of parameters used in the model, but the general picture does not. In Figure 13, only approximate values of energy are given. The four lowest excited configurations lie at about 3 eV and involve promotion of an electron from one of the two almost degenerate highest occupied orbitals into one of the lowest two empty orbitals. In the D_{2h} symmetry group, two of the configurations are of B_{1u} symmetry and two of B_{2u} symmetry. The next group of eight singly excited configurations is considerably higher in energy (ca. 6 eV) and they are all of A_g and B_{3g} symmetries, as is a group of 10 doubly excited configurations which have similar energies (5–7 eV). The next higher group of configurations of the "allowed" B_{1u} and B_{2u} symmetries is found only at energies near 7 eV.

Now, when configuration interaction (CI) is introduced in order to estimate final state energies, "plus" and "minus" states will result. Here, we use a well-known terminology due to Pariser.[20] The lowest four configurations give rise to three plus states and one minus state, whose calculated order is independent of details of the procedure: B_{1u}^- (L_b) at lowest energy, then the two B_{2u}^+ states (L_a below B_a), then B_{1u}^+ (B_b). Calculated mixing with higher energy B_{1u} and B_{2u} configurations is very small. A large number of A_g and B_{3g} states is also predicted, near or above the highest of the four states just discussed.

We have performed numerous π-electron calculations of the PPP type with different approximations for electron repulsion and resonance integrals and different assumed geometries for the perimeter, but the results were the same, except for the order of the almost degenerate B_{2u}^+ (B_a) and B_{1u}^+ (B_b) states, which depends on the shape of the ring. In particular, we have employed large-scale CI with up to 140 configurations selected from all 1225 doubly excited configurations by automatic inspection of the matrix elements of the Hamiltonian using a method described in detail elsewhere.[21] The results can be summarized as follows: The PPP model predicts unequivocally that the lowest two electronic transitions are into a B_{1u}^- (L_b) state (forbidden by the plus-minus selection rule[20] within the simple PPP model) and into a B_{2u}^+ (L_a) state (about 5000 cm^{-1} higher in energy, y-polarized, and much stronger). Also, almost certainly, the third transition is into a B_{2u}^+ (B_a) state and is y-polarized and reasonably intense. This is followed closely by a very strong z-polarized transition into a B_{1u}^+ (B_b) state surrounded by close to a dozen forbidden transitions into A_g and B_{3g} states, whose order is quite uncertain. In Clar's nomenclature, $L_b = \alpha$, $L_a = p$, $B_b = \beta$, $B_a = \beta'$. Two examples of numerical results are shown in Table III. One uses all singly excited configurations and the Mataga–Nishimoto approximation[22] for electron repulsion integrals, the other uses 28 singly and 104 doubly excited configurations selected by the SECI-1 procedure[21] from all 1225 doubly excited configurations and semiempirical parameters appropriate[23] for extensive CI. The use of these parameters[23] requires a compensation for the absence of highly excited configurations in the calculation in that the SCF energy rather than the CI energy is to be taken for the energy of the ground state and this was done in Table III (but not in Figure 14 where only trends are displayed, see below).

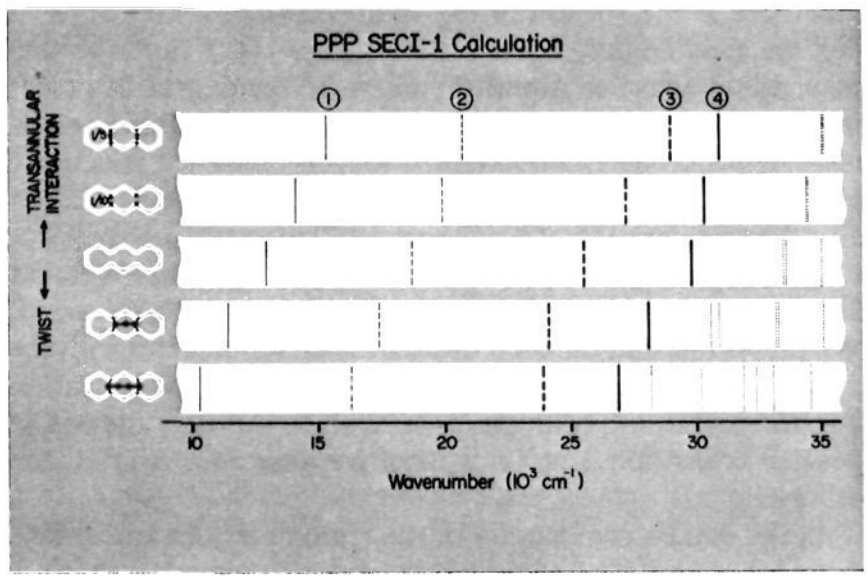

Figure 14. Calculated energies, intensities (thick line, intense; thin line, weak), and polarizations (full line, long-axis; dashed line, short-axis; dotted line, symmetry-forbidden) of electronic singlet–singlet transitions. Center line: planar [14]annulene VI. Above: resonance integrals for transannular bonds added ($\frac{1}{10}$ and $\frac{1}{5}$ the magnitude of these along the perimeter). Below: resonance integrals reduced according to twist angles observed in the butano-[12] and propano-[13] bridged annulenes I and II.

b. Bridged Annulenes. The actual compounds I–IV differ from hypothetical VI in several important respects. First, the 14-membered ring is distorted from planarity. From x-ray data[13,14] and molecular models, the nonplanarity decreases regularly as one goes from I to V. It is already quite small in III and IV. Second, various bonds in the 14-membered ring are twisted, so that the π-bonds between neighbors are weakened in various places along the periphery. The twisting is most severe in I, less so in II, even less in III and IV, whose models are quite similar, and is absent in V. The twist angles obtained from x-ray data[13,14] are shown in formulas I and II. Third, the twisting in I–IV also introduces "homoaromatic" transannular interactions between bottom lobes of atomic orbitals located on opposite sides of the bridge, leading to two quasi cyclopropano subunits in each molecule (dotted lines in formulas I–IV). Models indicate that the importance of this transannular overlap decreases along the series on going from I to IV. Fourth, in addition to imposing constraints on the geometry of the peripheral ring, the bridge may also exert inductive and hyperconjugative effects. One would suspect the latter to be particularly important in IV, where the occupied Walsh orbital of cyclopropane can efficiently interact with the annulene ring system, as shown by photoelectron spectroscopy.[7] Of course, in V, the bridge becomes an integral part of the total 16 π-

electron system which is effectively conjugated throughout. Similar but probably weaker interactions could be present in the other bridged annulenes I–III.

A proper interpretation of the spectra of the bridged annulenes would require either a prohibitively expensive ab initio calculation or, at least, a still quite expensive calculation by one of the all-valence electron semiempirical methods. Among standard methods, CNDO/S or INDO/S appear most attractive. However, we do not think the return would be worth the expense, both because neglect of overlap does not seem appropriate for a twisted π-electron system (cf. arguments outlined by Baird[24]) and because a large number of doubly excited configurations are present at relatively low energies already in the π-calculation (Figure 13). These would not be included in the standard CNDO/S procedure, and their inclusion would probably require complete reoptimization of parameters if a reasonable agreement with experiment were desired.

Instead, we have opted for the inexpensive use of simple concepts based on simulation of the various effects of the bridge within the PPP π-electron framework, and leave all-valence electron calculations on I–IV outside the scope of this paper. An added advantage of this simple approach is its ability to dissect the overall spectral changes into contributions from individual "effects" in a manner so often found useful by the organic chemist. Such a separation into effects is valuable in providing simple concepts transferable to other molecules. A similar attitude has been taken by Heilbronner et al.[7] in analyzing the photoelectron spectra of compounds I–V. In the simple model, distortions from planarity and bond twisting are simulated by changing the values of appropriate resonance integrals (decreased overlap of 2p AO's). Transannular interaction is simulated by adding new nonzero resonance integrals between appropriate pairs of atoms and inductive effect of the bridge by changing the one-center parameters for the carbon atoms which carry the bridge. Hyperconjugation is more difficult to mimic reliably in a simple manner; here, comparison with the fully conjugated planar hydrocarbon V will provide some feeling for what the effects might be. Any one of these effects, or any combination of several of these, can thus be studied easily, whereas in experiments or in sophisticated calculations, they are all present simultaneously to varying degrees so that their relative importance and even direction would be hard to deduce unequivocally.

Transitions 1–4. We start by noting that, in spite of minor differences between compounds I to IV, the energies, polarizations, and intensities of these four transitions generally fit well the requirements for the four symmetry-allowed transitions expected for VI (Figure 12, Tables II, III). Therefore, in the C_{2v} group, we assign the excited state of transition 1 as B_1, those of transitions 2 and 3 as B_2, and that of transition 4 as B_1, and postulate that they correlate with the B_{1u}^- (L_b), B_{2u}^+ (L_a), B_{2u}^+ (B_a), and B_{1u}^+ (B_b) states of VI, respectively. This implies that the short-axis polarized transitions 2 and 3 are polarized along y in formulas I–IV.

In order to explain the decrease in the energies of these transitions on going from I to IV (Figure 12), we have performed numerous simple π-electron calculations of the type just discussed, and conclude that the observed trend results from two opposing major contributions (Figure 14). The first of these is bond twisting. The pattern of π-bond weakening due to the twisting is established from x-ray studies[13,14] and is shown in formulas I and II. Its effect is to decrease the excitation energy on going from VI to I, just the opposite of what is observed. The direction of this effect may be surprising at first sight, but is easily understood if one permits the twisting to proceed to its limit, namely 90°, for the four bonds which twist the most. The perimeter is then broken up into two butadiene units and two allyl radicals and thus should have very

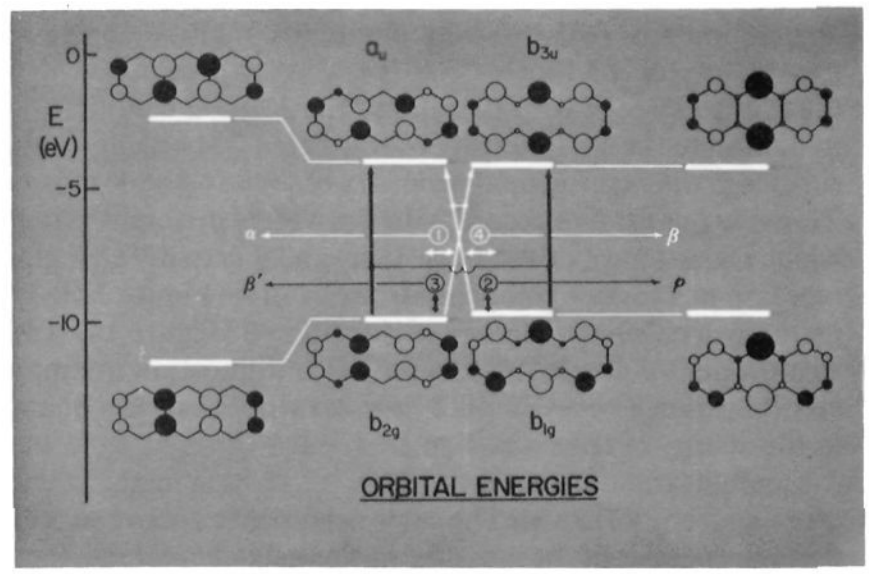

Figure 15. Center: frontier molecular orbitals of [14]annulene (VI). Right and left: their conversion to orbitals of anthracene (VII) by introduction of transannular interaction. Assignment of one-electron excitations to singlet–singlet transitions in VI and VII is shown. White lines: long-axis polarized transitions; black lines: short-axis polarized.

low-lying excited states (two nonbonding orbitals occupied by a total of two electrons in the ground state, a "biradicaloid" species[25]).

The opposing effect, which prevails and establishes the observed experimental trend, is homoaromatic transannular interaction. It acts to increase the calculated excitation energy of transitions 1–4 on going from VI to I. Carrying it again to its logical extreme by permitting the transannular interactions to be just as strong as those between bonded neighbors will convert the π-system of VI into that of anthracene (VII). This shows that transition 1 correlates with the L_b (α) transition of anthracene which seems to have so far eluded definitive experimental observation,[26] while transitions 2, 3, and 4 correlate with its well-known transitions L_a (p), B_a (β'), and B_b (β), as shown in Figure 12. This correlation easily explains the direction of the observed trends in excitation energies in the series I–IV.

Figure 15, based on standard PPP calculations, shows the origin of the correlation in simple MO terms. In the center are displayed the four frontier orbitals of VI (2, b_{2g}; 1, b_{1g}; −1, b_{3u}; −2, a_u) and the four single electron promotions which yield the four configurations which enter the excited states of transitions 1–4: 1 → −2 and 2 → −1 mix in equal proportions to give the excited states of transitions 1 (out-of-phase combination, minus state) and 4 (in-phase combination, plus state), 1 → −1 and 2 → −2 mix in roughly equal proportions to give those of transitions 2 (in-phase combination, 2 → −2 somewhat more important, plus state) and 3 (out-of-phase combination, 1 → −1 somewhat more important, plus state). Bonding orbitals are numbered 1, 2, . . . in the order of decreasing energy, and antibonding ones −1, −2, . . . in the order of increasing energy. Introduction of resonance integrals across the ring affects the energies of these four orbitals to varying degrees and transforms them into those of VII, as shown on the right and left. This converts the four singly excited configurations into the four well known to be involved in anthracene L_b, L_a, B_b, and B_a excited states. Orbitals 1 and −1 have very small expansion coefficients at the carbons where the transannular interaction takes place, and as a result, remain almost unaffected on going to VII. Configuration 1 → −1, now mixed only very little with 2 → −2, becomes the L_a (p) plus state of anthracene, while 2 → −2, mixed with very little 1 → −1, becomes its B_a (β') plus state. Since orbitals 1 and −1 remain almost unchanged on going from VI to VII, the energy of configuration 1 → −1 also remains almost constant. On the other hand, the separation of orbitals 2 and −2, and thus also the energy of configuration 2 → −2, increases dramatically. Already a transannular res-

onance integral equal to only one-tenth of those on the perimeter causes the $1 \rightarrow -1$ configuration to prevail heavily in the excited state of transition 1 and the $2 \rightarrow -2$ configuration to dominate the excited state of transition 2 (twisting the perimeter to the experimental geometry of I has the same effects). This is in qualitative accord with the widely different rates at which transitions 2 (almost constant) and 3 (rapidly changing) increase in energy upon going from I to IV (Figure 12). The increase in calculated energy of transition 2 (Figure 14) is due to a gradually decreasing degree of configuration mixing of configuration $1 \rightarrow -1$ with $2 \rightarrow -2$, rather than to a change in the energy of configuration $1 \rightarrow -1$.

Configurations $1 \rightarrow -2$ and $2 \rightarrow -1$ remain mixed equally on going from VI to VII. The same argument as above suggests that the energies of these configurations should increase faster than that of $1 \rightarrow -1$ but less than that of $2 \rightarrow -2$. Again, this agrees with the relative rates at which transitions 1 and 4 move in Figure 12 compared with transitions 2 and 3.

Thus, the series I–IV provides an interesting experimental demonstration of the perimeter model for the gradual construction of a polycyclic hydrocarbon by introduction of cross-links into an annulene. This concept has been established in theory since the classical work of Platt and Moffitt and serves as a basis for classification of electronic states of hydrocarbons.[27]

The existence of the "missing" L_b (α) band of anthracene can be inferred from its presence in anthracene derivatives with strongly perturbing substituents.[26] It is interesting that its existence has now also been documented by weakening the transannular bonds, i.e., going from VII to I. This shifts it to lower energies so that it is no longer covered up by the intense L_a band.

The effect of nonplanarity and the inductive effect of the bridge are calculated to play a subordinate but not totally negligible role. Some aspects of the inductive effect are worth noting, since we shall need to refer to them in the discussion of hyperconjugation and MCD spectra. To the first order, the effect of electron donation from the bridge raises orbital energies by amounts proportional to the squares of the expansion coefficients of the orbitals at the points of attachment. Inspection of the form of the orbitals (Figure 15) shows that orbitals 2 (b_{2g}) and -2 (a_u) are raised in energy by equal amounts, while the energy of orbitals 1 (b_{1g}) and -1 (b_{3u}) remains almost unchanged. Thus, the energies of configurations $1 \rightarrow -1$ and $2 \rightarrow -2$ remain essentially unchanged, and so does their balance in the excited states of transitions 2 and 3. We have already noted above that transannular interaction (as well as large twisting) causes the $1 \rightarrow -1$ configuration to predominate in excited state 2 and the $2 \rightarrow -2$ configuration to predominate in excited state 3. It is seen now that consideration of the inductive effect will not change this situation. On the other hand, the previously degenerate configurations $1 \rightarrow -2$ ($b_{1g} \rightarrow a_u$) and $2 \rightarrow -1$ ($b_{2g} \rightarrow b_{3u}$) are affected differently, so that their mixing in states 1 and 4 is unbalanced and the plus–minus pairing symmetry is broken. The energy of the $b_{2g} \rightarrow b_{3u}$ configuration is lowered, that of the $b_{1g} \rightarrow a_u$ configuration is increased. The former will then predominate in the excited state of the lower energy transition 1, the latter in that of the higher energy transition 4. The exact balance of the two opposing contributions provided by the two configurations to the transition moment of transition 1 will be destroyed, since the vector provided by configuration $2 \rightarrow -1$ will be longer than the opposing vector provided by $1 \rightarrow -2$. The transition acquires a weakly allowed character, in agreement with experimental observations. In the case of transition 4, whose excited state is represented by the in-phase combination of $2 \rightarrow -1$ and $1 \rightarrow -2$, the two vector contributions are adding up rather than subtracting and little change will be noted.

At this point, one wonders how serious is the so far neglected hyperconjugative effect of the bridge. At the same time, one wonders about the origin of transitions A, B, and C.

Transitions A–C. So far, we have been provided with no clue as to the relation of these transitions to those of [14]annulene VI. As already emphasized, even quite large CI calculations on VI fail to bring any additional calculated states substantially below that of transition 4, i.e., below ca. 30 000 cm^{-1}. It has been shown[28] that minus states are particularly likely to be shifted to lower energies as the full CI limit is approached, but even then, comparison with other quite extensive CI calculations on π systems of this size[23] leaves little if any hope that transitions A–C could be assigned to such minus states calculated to be at higher energies in Table III, since the discrepancy in the calculated and observed order of energies is excessive.

Inclusion of bond-twisting, transannular interactions (Figure 14), nonplanarity, and inductive effects in the π-electron calculation do not improve the situation. Transitions 1–4 remain the lowest and there is no evidence for states which could be correlated with transitions A–C. We conclude that these transitions are not simply related to π-electron states of [14]annulene VI. Their energies also appear to be too low for assignment to Rydberg states.

This leaves us with σ-electrons and the hyperconjugative effect of the bridge. There is, to our best knowledge, no safely established precedent for excited states significantly involving σ-electrons at such low energies in any hydrocarbon with "ordinary" structure (no radical centers, etc.). Although $\sigma \rightarrow \pi^*$ and $\pi \rightarrow \sigma^*$ transitions are generally believed to be present in the spectra of π-electron chromophores, they are thought to occur at high energies and to be covered by stronger π–π^* bands, and have never been assigned in spectra of chromophores containing two or more conjugated double bonds. Of course, since the hydrocarbons I–IV are non-planar, they represent a particularly favorable case for observation of low-energy states involving heavy σ–π mixing. Indeed, strictly speaking, they have no σ and π orbitals, unlike the planar species V, VI, and VII.

We believe that a clue to the assignment of the origin of transitions A–C is provided by comparison with the spectra of the planar 16 π-electron hydrocarbon V, in which the bridge is fully conjugated with the perimeter. These have been published[5] and are reproduced in Figures 5 and 11, since comparison of spectral detail appears crucial. From striking similarities of band shapes, energies, intensities, and polarizations, it is tempting to draw parallels between the transitions in I–IV and those in V, and to attach labels 1–4 and A–C to transitions of V as shown in Figure 5 and 11. The similarities are compelling and assignment straightforward in all cases except transition B, which cannot be identified in V in the spectral region in which it occurs in III and IV, and perhaps also in I and II. However, there is an additional weak band at low energies in V, assigned tentatively as B in Figures 5 and 11. The MCD spectra of I–IV on the one hand, and V on the other, are not similar, except for transitions 3 and 4, but this is perhaps not surprising considering the sensitivity of MCD spectra to minor perturbations, already mentioned above.

The symmetries of the excited states of transitions 1–4 in the annulenes I–IV agree with the known[5] symmetries of the corresponding excited states in V. The situation is less clear-cut for transitions A–C. In V, transition assigned as B is symmetry-forbidden[5] (A_g or B_{3g} excited state), transitions A and C appear long-axis polarized (B_{1u}), but the very weak transition A could actually be symmetry-forbidden and borrow its intensity through vibronic interactions. The calculated symmetries for the states of V are all compatible with the experimental results: A, A_g; B, B_{3g}; C, B_{1u}. The calculated but unobserved states of V are a B_{3g} state between states 2 and C and an A_g state between states 3 and 4. If we assume that the

computed symmetries of states A–C in V are correct, and if our correlation with the states of I–IV is valid, the symmetries of these states in the bridged annulenes I–IV should be: A, A_1; B, A_2; C, B_1. Thus their purely electronic polarizations should be: A, along x; B, forbidden; C, along z. Experimentally, in I–IV, transitions A and C appear with z-polarized intensity, and B is short-axis polarized (y, or less likely, x). As already mentioned above, the very weak intensity of transition A could be of vibronic origin if the purely electronic intensity is zero by symmetry or close to zero by accident, and this might even be true of the somewhat stronger transition B.

Thus, it is only for the strong transition C that experiment unequivocally agrees with expectations based on the correlation of the bridged [14]annulenes I–IV with the 16 π-electron hydrocarbon V. For transition A, we must postulate an unobserved very weak 0–0 component with x-polarization and assign the very weak observed intensity to vibronic mixing. This is somewhat arbitrary but perhaps acceptable considering that III and IV are almost planar, so that any x-polarized intensity should be quite weak, while in the less planar I and II transition A is badly overlapped by transition 1. For transition B, we must postulate an unobserved symmetry-forbidden 0–0 component and assign the weak observed intensity to vibronic mixing. Again, this is arbitrary but quite plausible.

In summary, we feel that a correlation of states of I–IV with those of V is reasonably well established, although admittedly less than compelling. Unresolved questions remain for two of the seven transitions.

Now, it is significant that in the case of V there are no experimentally observed bands which would not be accounted for by π-electron calculations. Actually, as noted above, below the intense band at 35 000 cm^{-1} two more transitions are predicted than are observed, but both are calculated to be symmetry-forbidden and could easily be covered up by other transitions. Apparently, the interaction of the perimeter with the two π centers on the bridge has brought down in energy more than a sufficient number of excited states to account for all states observed. The manner in which this occurs is shown in Figure 16, based on standard PPP calculations,[19] in which the π-electron orbital energies of VI are shown on the left and those of ethylene in the center. Their mutual interactions are limited by symmetry and energy separations. As shown in Figure 16, very strong interactions occur only between the bonding π orbital of ethylene and the orbital 3 of VI (both of b_{3u} symmetry), and between the antibonding π^* orbital of ethylene and the orbital −3 of VI (both of b_{2g} symmetry). In both cases, mixing is almost one to one. The resulting π-electron energy levels of V are shown on the right. Our results agree completely with those computed by Batich, Heilbronner, and Vogel,[7] and with their assignment of peaks in the photoelectron spectrum of V. They also agree with the computations and assignments of Bischof and Gleiter[29] except for the order of the highest two occupied orbitals which these authors assign reversed (b_{3u} above b_{1g}). Since these are almost degenerate (Figure 16), their exact ordering matters little for our arguments. Like these two groups of authors,[7,29] we are not in agreement with the results calculated by Müllen and Reel.[30]

It is seen that the lowest two empty orbitals (−1, b_{3u} and −2, a_u) do not change much. Their calculated order in V is in agreement with an ESR study of the radical anion.[30] On the other hand, orbital −3 (b_{2g}) is considerably lower in energy in V, and looks much like the π^* (b_{2g}) orbital of ethylene with an in-phase admixture of one of the perimeter orbitals (b_{2g}, −3 in VI). Changes are even more dramatic among occupied orbitals of VI. The highest among these (1, b_{1g}) has a nodal plans through both atoms of the ethylene bridge and therefore is not affected on going to V, but the next one (2, b_{2g}) interacts with the π^* (b_{2g}) orbital of ethylene and becomes much more bonding, so that it is only no. 3 in V, while no. 2 (b_{3u}) is an orbital consisting mostly of the bonding π (b_{3u}) component of the ethylene bridge combined out-of-phase with one of the perimeter orbitals of VI (b_{3u}, 3 in VI). As a result of these changes, one can expect qualitatively that the energies of the low-lying configurations already present in VI, and therefore the energies of the states which they represent, will be affected.

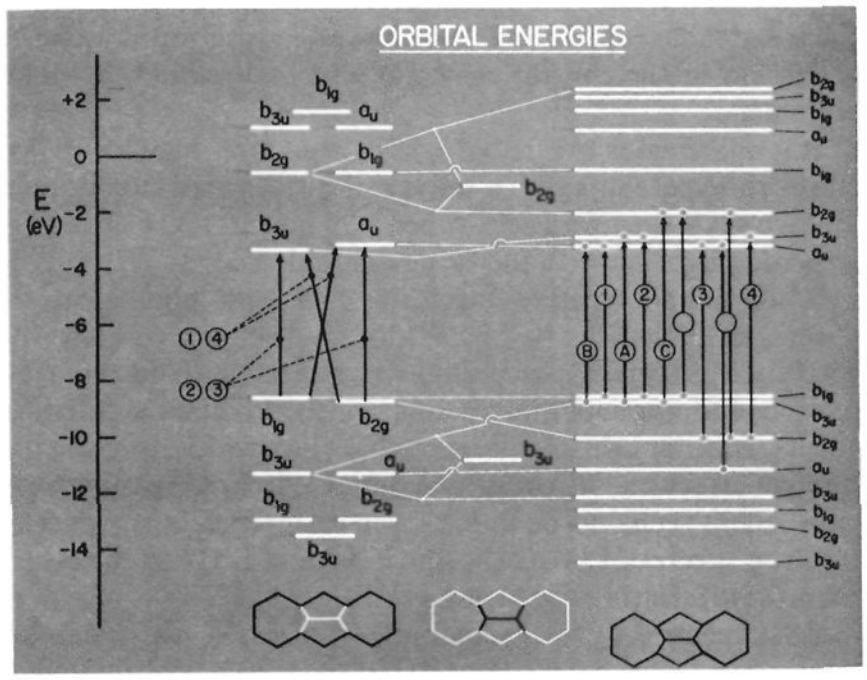

Figure 16. Molecular orbitals of [14]annulene (VI), ethylene, and their interaction yielding the orbitals of dicyclohepta[*cd,gh*]pentalene (V) (PPP approximation). Assignment of one-electron excitations to observed transitions in V is shown. Empty circles indicate transitions which are predicted but have not been observed. A constant correction of +1.6 eV needs to be added to the computed orbital energies to bring them into correspondence with experimental results for V[7] using Koopmans' theorem.

Introduction of the ethylene bridge into the alternant hydrocarbon VI to give the nonalternant V obviously destroys pairing symmetry and plus–minus classification of states. On going from VI, the energy of configurations $1 \rightarrow -1$ ($b_{1g} \rightarrow b_{3u}$) and $1 \rightarrow -2$ ($b_{1g} \rightarrow a_u$) does not change much, but that of configurations $2 \rightarrow -1$ ($b_{2g} \rightarrow b_{3u}$) and $2 \rightarrow -2$ ($b_{2g} \rightarrow a_u$) increases considerably. As a result, in V configuration $1 \rightarrow -2$ ($b_{1g} \rightarrow a_u$) dominates the excited state of transition 1, which now has quite respectable intensity, while configuration $2 \rightarrow -1$ ($b_{2g} \rightarrow b_{3u}$) prevails in the excited state of transition 4, which is shifted to higher energies. Also the approximate balance of configurations $1 \rightarrow -1$ ($b_{1g} \rightarrow b_{3u}$) and $2 \rightarrow -2$ ($b_{2g} \rightarrow a_u$) in excited states of transitions 2 and 3 no longer exists. The former prevails in the excited state of transition 2, the latter in that of transition 3, which is also shifted to higher energies.

More important, new transitions should appear on going from VI to V, since V has an additional high-lying occupied orbital (2, b_{3u}) and an additional relatively low-lying empty orbital (−3, b_{2g}). Indeed, according to the calculations, transitions A, B, and C in V all involve excitations from the new high-lying orbital (2, b_{3u}): A, into orbital −2 (b_{3u}); B, into −1 (a_u); C, into −3 (b_{2g}). Since the new high-lying orbital 2 (b_{3u}) has large amplitude on the atoms of the central ethylene bridge, whereas orbitals −1 (a_u) and −2 (b_{3u}) do not, transitions A and B involve partial charge transfer from the ethylene bridge to the periphery. Transitions from orbital 1 (b_{1g}) to −3 (b_{2g}) and from 3 (b_{2g}) to −3 (b_{2g}) are also predicted to appear at relatively low energies, but as already mentioned, are symmetry-forbidden and presumably not observed.

We propose that in compounds I–IV the orbitals of the saturated bridge act similarly, albeit more weakly, as the ethylene orbitals in Figure 16, and in this way bring about the low-energy excitations A, B, and C. Of course, it appears certain that for compounds I and II, in which the two bridging carbon atoms are not directly bonded to each other, V is less

suitable as a model than it is for III and IV, and the hypothetical double heptafulvene which would result formally from a scission of the central ethylene unit in V would be more suitable.

It is unorthodox to attribute the existence of three low-lying states to hyperconjugative effects of a saturated substituent and we shall therefore seek other evidence in favor of strong hyperconjugation with the bridge in molecules I–IV.

Some support comes from the fact that photoelectron spectra of molecules I–V have already been interpreted[7] by reference to these hyperconjugative effects, with due consideration of transannular interaction, which also helps to stabilize the b_{2g} frontier orbital relative to b_{1g} (Figure 15), and the inductive effect and effect of twisting. Compared with our results, there seems to be much more difference in the photoelectron spectra of IV on the one hand and I–III on the other than there is within the group I–III.

ESR spectra[8] of the radical anions of I–IV, which can be interpreted to give information about the lowest free molecular orbital in I–IV, cannot be expected to reveal the presence of hyperconjugative effects of the bridge. As seen in Figure 16, even in the limiting case of V itself, the effect of the central bridge barely splits the almost degenerate antibonding frontier orbitals, placing b_{3u} a little above a_u. On the other hand, transannular interaction pushes a_u above b_{3u} (Figure 15) and should easily overwhelm the anticipated feeble hyperconjugative effect of the bridge. Indeed, experimentally, b_{3u} is below a_u in I–IV,[8] and a_u is below b_{3u} only in the fully conjugated V.[30] Consideration of the inductive effect, which destabilizes the b_{2g} frontier orbital with respect to b_{1g} and a_u with respect to b_{3u}, also accounts for the experimental result.[8]

It would be somewhat more helpful to obtain the ESR spectra of the radical cations of I–IV. The inductive effect would favor b_{2g} as the highest occupied molecular orbital, hyperconjugation favors b_{1g}. Unfortunately, the effect of transannular interaction, whose presence is quite firmly established both from PES work[7] and the present study (Figures 12, 14), also is to favor b_{1g}, and the two effects would be hard to separate. The ESR spectrum would then mainly serve as a support for the PES assignment.

One type of observation in which the otherwise ubiquitous interfering effects of transannular interaction are conspicuously absent is a study of deviations from perfect pairing symmetry. This symmetry is not disturbed by twisting and transannular interaction, since they still leave the system alternant, but is destroyed by the inductive and hyperconjugative effects, as already discussed. Of course, even in VI, the pairing symmetry is only approximate since the PPP model itself is only approximate, but it is well known what order of magnitude to expect as a result of the imperfection of the PPP model (cf. the extremely small but nonzero intensity of transitions into minus excited states in alternant hydrocarbons).

The best known consequence of a loss of perfect pairing symmetry is increased intensity of transitions into minus excited states, in our case transition 1, and we have already pointed out that the observed intensity can be attributed to either an inductive or a hyperconjugative effect of the bridge. It is interesting to note that the two perturbations work at cross-purposes. Hyperconjugation makes the energy of the $1 \rightarrow -2$ ($b_{1g} \rightarrow a_u$) configuration lower than that of the $2 \rightarrow -1$ ($b_{2g} \rightarrow b_{3u}$) configuration, so that the excited state of transition 1 is of prevailing $1 \rightarrow -2$ nature and nonzero intensity results since the vector contributed by the $1 \rightarrow -2$ component of the excited state is longer than the opposing vector contributed by the $2 \rightarrow -1$ component. The inductive effect works in just the opposite direction, making the $1 \rightarrow -2$ energy higher than $2 \rightarrow -1$. The stronger of the two effects will prevail and impose either predominant $1 \rightarrow -2$ or predominant $2 \rightarrow -1$ character on the excited state of transition 1. It is not likely that the two mechanisms would exactly cancel each other's effects, although one can see some signs of partial cancellation in the very small oscillator strengths of transition 1 in I and II compared with higher intensities in III and IV (Table II): perhaps the hyperconjugative effect prevails strongly in III and IV and only weakly in I and II. However, since observed intensities only depend on the length of the transition moment vector and not on its sense (along the positive or negative direction at the z axis, given a particular choice of orbital phases), they are clearly unsuitable for unravelling the mechanism by which a nonzero value arose, i.e., whether $1 \rightarrow -2$ or $2 \rightarrow -1$ is the prevailing configuration in the excited state of transition 1.

Another manifestation of a loss of perfect pairing symmetry is the increased intensity in MCD spectra. The PPP model predicts zero B terms for all transitions for a system with perfect pairing[17] and the observed nonzero values can then be taken as a measure of deviation from such a system, ascribable either to the imperfection of the PPP model, or to a loss of perfect pairing symmetry within the model, say due to inductive or hyperconjugative substitution. For a variety of π-electron systems without perfect pairing, signs of B terms predicted by the simple PPP model are in very good agreement with experiment[5,9,10,16] (cf. Figure 11), and it seems reasonable to attempt an interpretation of the signs observed in compounds I–IV on the basis of the PPP model, considering them as slightly perturbed [14]annulene VI.

MCD spectroscopy is well suited for answering the type of question posed here; i.e., does transition 1 acquire nonzero intensity because the $1 \rightarrow -2$ configuration dominates over $2 \rightarrow -1$ in its excited state or because the $2 \rightarrow -1$ configuration dominates over $1 \rightarrow -2$? This is because the signs of B terms depend not only on lengths of transition moment vectors, but also on their sense. A general difficulty is that the B term of a transition $G \rightarrow F$ contains contributions from magnetic mixing of all other states I into both G and F. As is discussed in detail in ref 16a, it is often possible to neglect all but one of these contributions, since strong mixing of I into F requires a small energy difference between them (mixing of I with G is rarely important since the energy difference is usually too large), large intensities for transitions $G \rightarrow F$ and $G \rightarrow I$, and mutually perpendicular polarization for these two transitions. The situation is clearly not favorable for an analysis of the B term of transition 1 in I–IV, since interactions of its excited state with those of transitions 2, 3, and B can all be important. However, the B terms of transitions 3 and 4 are not only stronger than others, but also approximately equal in magnitude and of opposite signs, the transitions are intense, very close in energy, and polarized perpendicular to each other, so that there is little doubt that the observed signs of their B terms are dominated by their mutual mixing by the magnetic field. Indeed, in a [14]annulene of D_{14h} symmetry, the two transitions would be degenerate and subject to a first-order Zeeman effect. We shall now use the signs of the B terms to determine whether the configuration $1 \rightarrow -2$ or $2 \rightarrow -1$ prevails in the excited state of transition 4. The other one will then prevail in that of transition 1 and the above posed question will be answered.

Refering to ref 16a for details and literature sources, we note that the positive sign of the B term of the lower transition 3 and negative sign of the B term of the higher transition 4 imply that the sign of the triple vector product $(1/i)\langle 3|\boldsymbol{\mu}|4\rangle \cdot \langle G|\mathbf{m}|3\rangle \times \langle 4|\mathbf{m}|G\rangle$ must be positive. Here, i is the imaginary unit, $\langle 3|\boldsymbol{\mu}|4\rangle$ is the magnetic dipole transition moment vector for transition from excited state 3 to excited state 4, $\langle G|\mathbf{m}|3\rangle$ and $\langle 4|\mathbf{m}|G\rangle$ are the electric dipole transition vectors for transitions from the ground state to excited states 3 and 4, respectively. Using the choice of orbital phases indicated in Figure 15 and the PPP calculations discussed previously, the excited states of transitions 3 and 4 can be adequately represented by linear combinations of configurations $K_1 \cdot (1 \rightarrow -1) - K_2 \cdot (2 \rightarrow -2)$ and

$K_3\cdot(1 \rightarrow -2) + K_4\cdot(2 \rightarrow -1)$, respectively, where all K's can be taken to be positive. As already discussed, K_1 and K_2 are about the same in VI, but the effects of transannular interaction, twisting, and hyperconjugation present in I–IV all make K_2 larger than K_1 (the inductive effect is not opposed to this ordering, but does not promote it, either). Thus, there seems to be no doubt that $K_2 > K_1$, and this is also supported by PES results[7] which show that orbital 2 is more stable than orbital 1 by several tenths of an eV. In a system with perfect pairing, $K_3 = K_4$, and this holds for I–IV unless the inductive and hyperconjugative effects are considered. If the inductive effect dominates, the configuration $1 \rightarrow -2$ prevails in the excited state of transition 4 and $K_3 > K_4$; if hyperconjugation dominates, the configuration $2 \rightarrow -1$ prevails and $K_3 < K_4$.

The direction of the vector product $\langle G|\mathbf{m}|3\rangle \times \langle 4|\mathbf{m}|G\rangle$ in molecules I–IV is easily derived from consideration of the transition densities derived by inspection of Figure 15. It points away from the reader, below the plane of paper. Since the triple vector product is positive, it follows that for the given choice of orbital phases the vector $(1/i)\langle 3|\mu|4\rangle$ also points below the plane of paper. Substituting for the wave functions of the excited states, using $\langle s \rightarrow t|\mu|u \rightarrow v\rangle = \langle t|\mu|v\rangle\delta_{su} + \langle s|\mu|u\rangle\delta_{tv}$, and $\langle s|\mu|t\rangle = \langle -t|\mu| -s\rangle$, where s, t, u, and v are labels of molecular orbitals (cf. ref 17), we get $\langle 3|\mu|4\rangle = (K_2 - K_1)(K_4 - K_3)\langle 2|\mu|1\rangle$.

Since $K_2 - K_1 > 0$, it follows that the vector $[(K_4 - K_3)/i]\langle 2|\mu|1\rangle$ points below the plane of paper. It is clear that the vector would have zero length and provide no contribution to the B term in the case of perfect pairing ($K_3 = K_4$) and that, in principle, it could have either direction depending on which of K_4 and K_3 is bigger, i.e., depending on the relative importance of the inductive and hyperconjugative effects. Thus, it is obvious how a weak perturbation can determine the signs of the B terms of an alternant hydrocarbon, in accordance with the known[18] sensitivity of the MCD spectra of the annulenes to structural details. A similar simple analysis can be performed for alternant hydrocarbons in general and has been published separately.[31]

The direction of the vector $(1/i)\langle 2|\mu|1\rangle$ is easy to obtain by inspection of the molecular orbitals using methods of ref 16a. In units of Bohr magnetons,

$$(1/i)\langle 2|\mu|1\rangle = 0.131\,|\beta_{\mu\nu}| \sum_{\substack{\text{bonds}\\ \mu,\nu}} \mathbf{R}_\mu \times (c_{\mu 2}c_{\nu 1} - c_{\nu 2}c_{\mu 1})(\mathbf{R}_\nu - \mathbf{R}_\mu)$$

where $\beta_{\mu\nu}$ is the resonance integral between atoms μ and ν, the sum is over all bonds, the terminal atoms of the bonds have position vectors R_μ and R_ν, and $c_{\lambda i}$ is the expansion coefficient at λth atom in ith molecular orbital. Inspection of Figure 15, which displays the expansion coefficients of orbitals 2 (b_{2g}) and 1 (b_{1g}) of VI shows that $(1/i)\langle 2|\mu|1\rangle$ is pointed below the plane of paper. It follows that $K_4 - K_3 > 0$, i.e., the configuration $2 \rightarrow -1$ prevails in the excited state of transition 4, $1 \rightarrow -2$ prevails in that of transition 1, and this implies that the hyperconjugative effect dominates over the inductive effect.

If the hyperconjugative effect determines the signs of the B terms of transitions 3 and 4 in I–IV, those signs should be the same in the fully conjugated hydrocarbon V, and this is indeed the case (Figures 7 and 11), cf. ref 5.

We find it satisfying that the hyperconjugative effect, which was postulated in I–IV in order to account for photoelectron spectra[7] and for the observation of transitions A, B, and C above, is now seen to be the only one of those we could think of which accounts for the quite independent observation of absolute signs in MCD spectra. Within the framework of the simple model used in our discussion, in which I–IV are viewed as perturbed [14]annulene, hyperconjugation with the bridge is clearly very important.

c. Comparison with VIII, a Bridged [14]Annulene with Pyrene Perimeter. The electronic absorption spectrum and polarized fluorescence of VIII and some of its simple derivatives were investigated some time ago by Heilbronner and collaborators.[32] They identified the four transitions which originate in the four low-lying symmetry-allowed $\pi \rightarrow \pi^*$ transitions of the 14π-electron perimeter, corresponding to our transitions 1–4, and established their relative polarizations. Simple calculations of the PPP type were in good qualitative agreement with the results and were used to derive the absolute polarizations and assign the transitions, in the order of increasing energies, as L_b (z-polarized, 15 600 cm^{-1}), L_a (y-polarized, 21 400 cm^{-1}), B_b (z-polarized, 26 500 cm^{-1}), B_a (y-polarized, 29 600 cm^{-1}). Here, we choose the z and y directions in formula VIII to cut through bonds and atoms of the perimeter, respectively, as they do in compounds I–VII, although in stretched sheet work on VIII, our normal labeling would be the opposite. The calculated estimates of the inductive and hyperconjugative effects of the saturated bridge in VIII on the transition energies were quite small. Our results are in perfect accord with the previous work and indirectly confirm the absolute polarizations deduced by Heilbronner et al.[32] Perhaps the only noteworthy remark concerns the inversion of the order of the B_b and B_a states in I–IV on the one hand and VIII on the other. These are expected to be degenerate in [14]annulene of D_{14h} symmetry and are calculated to split on going to D_{2h} symmetry if mutual repulsion of electrons on nonneighboring AO's is considered:[32] when the distortion is towards pyrene-shaped perimeter, B_b should lie below B_a, as indeed observed by Heilbronner et al.;[32] when it is towards an anthracene-shaped perimeter, B_a should lie below B_b, just as found in the present work. Our calculations also reproduce this trend and are in good numerical agreement with excitation energies observed in VIII.

Finally, it should be noted that an unassigned weak transition analogous to our transition A was observed in VIII.[32] The experimental data do not exclude the presence of additional transitions which might correspond to our transitions B and C. A possibility was discussed[18,33] that a similar additional band may also be generally present in the spectra of bridged [10] and 14]annulenes, and that it might be related to charge transfer from the bridge to the π system in the case of oxido and amino bridges. We believe that our results leave no doubt about the existence of low-energy transitions involving the σ-orbitals of the aliphatic hydrocarbon bridge, and make it likely that these correspond to partial charge transfers from a high-lying occupied σ-orbital of the bridge into low-energy orbitals of the π system.

Summary

In conclusion, it has been shown that the series of bridged [14]annulenes I–IV can be considered as a concrete illustration of the gradual transition from a hypothetical planar [14]-annulene VI to anthracene VII by introduction of cross-links, which has been long familiar in theory in connection with Platt's classification of electronic states of polycyclic hydrocarbons and Moffitt's discussion of the effects of the transannular bonds.[27] Moreover, the considerable spectral detail revealed by a combination of several spectroscopic techniques permitted us to identify additional excited states which cannot be simply related to the π states of VI without explicit consideration of the hyperconjugative effect of the saturated bridge. These states, probably also present in other bridged annulenes and previously tentatively detected there by other authors,[32] apparently represent the first instances in which "σ–π mixing" has led to appearance of new states in the low energy region (below 35 000 cm^{-1}). The postulated hyperconjugative effect of the bridge is also in accord with the observed absolute signs of the most intense bands in the MCD spectra of I–IV.

However, the present study cannot be considered definitive. First, certain plausible but unproven assumptions had to be made about detailed structure of two of the seven electronic bands studied. Investigations of related molecules, high resolution work, and possibly two-photon laser spectroscopy are called for. Second, high-quality calculations for I–IV are presently not available and must await the development of cheaper and/or better quantum mechanical procedures.

As a by-product, we have also obtained interesting information about the orientation of the nonplanar molecules I–IV in a stretched polymer. Finally, we have found some indications that the eclipsed central part of the butano bridge in 1 twists in the lowest excited state.

Acknowledgment. This work was supported by the National Science Foundation (Grant No. GP-37551). J. M. acknowledges support from the Alfred P. Sloan Foundation. We are grateful to Mr. M. R. Whipple and Miss P. L. Case for recording the MCD spectra, and to Professor H. Eyring for kindly providing us with access to his MCD instrument. Helium gas was provided by a departmental grant from the Office of Naval Research.

References and Notes

(1) (a) University of Utah; (b) presented at the 2d International Symposium on the Chemistry of Non-Benzenoid Aromatic Compounds, Lindau, Germany, Sept 23–27, 1974; (c) University of Cologne.
(2) N. L. Allinger, J. T. Sprague, and T. Liljefors, *J. Am. Chem. Soc.*, **96**, 5100 (1974), and references cited therein.
(3) H.-R. Blattmann, W. A. Böll, E. Heilbronner, G. Hohlneicher, E. Vogel, and J.-P. Weber, *Helv. Chim. Acta*, **49**, 2017 (1966).
(4) E. Vogel, W. Sturm, and H.-D. Cremer, *Angew. Chem., Int. Ed. Engl.*, **9**, 516 (1970); E. Vogel, A. Vogel, H.-K. Kübbeler, and W. Sturm, *ibid.*, 514 (1970); E. Vogel and H. Reel, *J. Am. Chem. Soc.*, **94**, 4388 (1972); H. Reel and E. Vogel, *Angew. Chem., Int. Ed. Engl.*, **11**, 1013 (1972); H. Reel, Dissertation, Universität Köln, 1972.
(5) V. Kratochvil, J. Kolc, and J. Michl, *J. Mol. Spectrosc.*, **57**, 436 (1975).
(6) A. Alscher, W. Bremser, D. Cremer, H. Günther, H. Schmickler, W. Sturm, and E. Vogel, *Chem. Ber.*, **108**, 640 (1975).
(7) C. Batich, E. Heilbronner, and E. Vogel, *Helv. Chim. Acta*, **57**, 2280 (1974).
(8) F. Gerson, K. Müllen, and E. Vogel, *J. Am. Chem. Soc.*, **94**, 2924 (1972).
(9) E. W. Thulstrup, P. L. Case, and J. Michl, *Chem. Phys.*, **6**, 410 (1974).
(10) J. Kolc, E. W. Thulstrup, and J. Michl, *J. Am. Chem. Soc.*, **96**, 7188 (1974).
(11) D. J. Shieh, S. H. Lin, and H. Eyring, *J. Phys. Chem.*, **77**, 1031 (1973).
(12) (a) E. W. Thulstrup, J. Michl, and J. H. Eggers, *J. Phys. Chem.*, **74**, 3868, 3878 (1970). (b) The theory described in ref 12a assumes that out-of-plane polarized absorption is negligible. A straightforward extension to the case of molecules with nonnegligible x, y, and z polarized transitions (E. W. Thulstrup and J. Michl, unpublished results) shows that $d_{\perp}{}^{\circ}$ and $d_{\parallel}{}^{\circ}$ can still be obtained exactly as before [and so can $K_1 = 1/(2d_{\perp}{}^{\circ} + 1)$ and $K_2 = d_{\parallel}{}^{\circ}/(2 + d_{\parallel}{}^{\circ})$]. In the case of uniform γ-distribution (equivalent short axes x and y), reduction yields the "pure" spectra A_z and $(A_x + A_y)$. This happens in the case of our molecules I–III. For inequivalent short axes (our molecule IV) exact reduction cannot be achieved from $E_{\parallel}$ and $E_{\perp}$ alone. In this case, the "long axis polarized" absorption curve in which features due to A_y have been reduced away will still contain spectral features due to transitions polarized along the other short axis, x, with relative weights $K_1 - K_2$ for A_z and $1 - K_1 - 2K_2$ for A_x. In the case of IV, the relative weights are about 1:(−1), but no features due to A_x are discernible, presumably because $A_z(\lambda) \gg A_x(\lambda)$. The "short axis polarized" absorption curve will contain contributions from both A_y (weight $K_1 - K_2$) and A_x (weight $2K_1 + K_2 - 1$). In the case of IV, the relative weights are about 1:2. However, since none of the peaks in this curve are shared with the "long axis polarized" curve (where they would appear negative), we again conclude $A_x \doteq 0$.
(13) C. M. Gramaccioli, A. Mugnoli, T. Pilati, M. Raimondi, and M. Simonetta, *Acta Crystallogr., Sect. B*, 28, 2365 (1972).
(14) A. Gavezzotti, A. Mugnoli, M. Raimondi, and M. Simonetta, *J. Chem. Soc., Perkin Trans. 2*, 425 (1972).
(15) D. J. Shieh, S. H. Lin, and H. Eyring, *J. Phys. Chem.*, **76**, 1844 (1972).
(16) (a) S. M. Warnick and J. Michl, *J. Am. Chem. Soc.*, **96**, 6280 (1974); (b) J. F. Muller, D. Cagniant, O. Chalvet, D. Lavalette, J. Kolc, and J. Michl, *ibid.*, **96**, 5038 (1974); E. W. Thulstrup, J. Michl, and C. Jutz, *J. Chem. Soc., Faraday Trans. 2*, **71**, 1618 (1975).
(17) J. Michl, *J. Chem. Phys.*, **61**, 4270 (1974).
(18) B. Briat, D. A. Schooley, R. Records, E. Bunnenberg, and C. Djerassi, *J. Am. Chem. Soc.*, **89**, 7062 (1967); B. Briat, D. A. Schooley, R. Records, E. Bunnenberg, C. Djerassi, and E. Vogel, *ibid.*, **90**, 4691 (1968).
(19) R. Pariser and R. G. Parr, *J. Chem. Phys.*, **21**, 466, 767 (1953); J. A. Pople, *Trans. Faraday Soc.*, **49**, 1375 (1953).
(20) R. Pariser, *J. Chem. Phys.*, **24**, 250 (1956).
(21) J. W. Downing, J. Michl, P. Jørgensen, and E. W. Thulstrup, *Theoret. Chim. Acta*, **32**, 203 (1974).
(22) N. Mataga and K. Nishimoto, *Z. Phys. Chem. (Frankfurt am Main)*, **13**, 140 (1957).
(23) J. W. Downing, Ph.D. Dissertation, University of Utah, 1974.
(24) N. C. Baird, *Mol. Phys.*, **18**, 39 (1970); *J. Chem. Soc., Chem. Commun.*, 199 (1970); cf. A. Warshel and M. Karplus, *J. Am. Chem. Soc.*, **94**, 5612 (1972).
(25) J. Kolc and J. Michl, *J. Am. Chem. Soc.*, **95**, 7391 (1973).
(26) J. Michl, E. W. Thulstrup, and J. H. Eggers, *Ber. Bunsenges. Phys. Chem.*, **78**, 575 (1974); D. M. Friedrich, R. Mathies, and A. C. Albrecht, *J. Mol. Spectrosc.*, **51**, 166 (1974), and references cited therein.
(27) J. R. Platt, *J. Chem. Phys.*, **17**, 484 (1949); W. Moffitt, *ibid.*, **22**, 320 (1954).
(28) J. Čízek, J. Paldus, and I. Hubač, *Int. J. Quantum Chem.*, **8**, 951 (1974).
(29) P. Bischof and R. Gleiter, "Topics in Non-Benzenoid Aromatic Chemistry", Vol. II, T. Nozoe, Ed., Halsted Press, New York, N.Y., in the press.
(30) K. Müllen and H. Reel, *Helv. Chim. Acta*, **56**, 363 (1973).
(31) J. Michl, *Chem. Phys. Lett.*, **39**, 386 (1976).
(32) H.-R. Blattmann, V. Boekelheide, E. Heilbronner, and J.-P. Weber, *Helv. Chim. Acta*, **50**, 68 (1967).
(33) W. Grimme, E. Heilbronner, G. Hohlneicher, E. Vogel, and J.-P. Weber, *Helv. Chim. Acta*, **51**, 225 (1968); see also ref 3.